Model Order Reduction Techniques for Simulation of Electromagnetic Systems with RLC Circuits

Takayuki WATANABE† and Hideki ASAI††

†School of Administration and Informatics, University of Shizuoka, 422-8526, Japan
(TEL/FAX: +81-54-264-5444, E-mail: watanat@u-shizuoka-ken.ac.jp)
††Dept. of Systems Engineering, Faculty of Engineering, Shizuoka University, 432-8561, Japan
(TEL/FAX: +81-53-278-1237, E-mail: hideasai@sys.eng.shizuoka.ac.jp)

Abstract: This paper describes model order reduction techniques for simulation of the electromagnetic systems with lumped RLC circuits. Especially, an efficient simulation method in the frequency domain is presented. This method models a printed circuit board (PCB) as a hybrid system of equations based on FDFD(Finite Difference Frequency Domain) method, which is composed of electromagnetic systems and RLC circuits. The model order reduction technique is utilized in order to construct the macromodels from the hybrid system of equations. Finally, the macromodels of power plane resonances on PCBs are generated and these macromodels are applied to the power plane resonance analysis of the PCB.

1. Introduction

In the design and signal integrity analysis of high-speed circuits, modeling LSI packages and printed circuit boards (PCBs) is one of the most important issues. For instance, the quasi-TEM transmission line model based on the telegrapher's equation is widely used as a model of interconnects. Because the transmission line models assume ideal ground planes, it can not simulate some important effects, such as the ground bounce. Furthermore, the actual PCBs and packages became multilayer with the increase of via-holes, the incomplete power/ground patterns and the complex line layout. If more accurate models are required, we need to model using the Maxwell's equations instead of the telegrapher's equation.

In order to perform the analysis in consideration of the detailed layout, the partial-element equivalent-circuits (PEEC) method, which models the whole PCB as numerous RLC lumped elements, has been widely used [1][2]. The PEEC network consisting of thousands of lumped elements is simulated efficiently by using a variety of model order reduction techniques as illustrated in Fig.1(a). In this method, the 3-dimensional extraction of lumped parameters, such as capacitances, self- and mutual- inductances, remains as a complicated problem and is computationally expensive.

As another method, the finite-difference time-domain (FDTD) method is one of the popular methods of analyzing scattering (S-) parameters between any pair of ports on the PCB because it uses a simple algorithm based on the finite deference method [3][4], unlike the Moment Method (MoM) and the Finite Element Method (FEM). The FDTD method can be connected to the SPICE-like circuit simulator, and perform transient analysis in synchronization. However the FDTD is based on the explicit algorithm and the time step size Δt is limited by the Courant condition. Therefore much more CPU time is required for the analysis of more refined structure. Here, the SPICE macromodel can be created by some techniques on the basis of least-squares method from the results obtained by the FDTD as illustrated in Fig.1(b) [5][6]. However, in particular, sampled data calculated by the FDTD method include some numerical noises. Therefore, it is difficult to preserve the passivity of the macromodel. Then, several methods of compulsorily enforcing the passivity of the macromodel have been proposed [7][8].

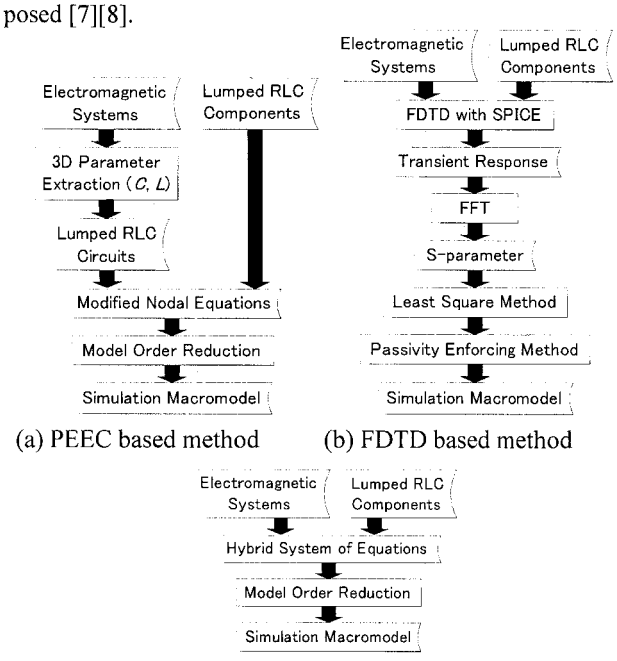

(a) PEEC based method (b) FDTD based method

(c) Proposed method

Fig. 1 Several macromodeling approaches.

In recent years, model order reduction techniques for electromagnetic systems have been proposed [9][10]. In these methods, the electromagnetic systems are formulated as the finite-difference frequency-domain (FDFD) equations, and reduced-order models are constructed by the passive and stable algorithms, such as the passive reduced-order interconnect macromodeling algorithm (PRIMA) [11] and the efficient nodal order reduction algorithm (ENOR) [12]. However, if we

intend to generate the macromodels for packages and PCBs mounting lumped components, such as decoupling capacitors, it is the best way to use the model reduction technique including not only electromagnetic systems but also lumped RLC circuits.

In this paper, an efficient macromodeling method of the hybrid systems, which are composed of electromagnetic systems and lumped RLC circuits, is proposed to overcome above problems. The proposed method extends the conventional electromagnetic model order reduction techniques to handle not only electromagnetic systems but also lumped RLC circuits. In the proposed method, electromagnetic systems are formulated as FDFD equations, and lumped RLC circuits are formulated as nodal equations. These equations are integrated into the hybrid system of equations as shown in Fig.1(c). Therefore, differently from the PEEC method, the technique presented here does not need any 3-dimensional capacitance and inductance parameter extraction techniques. Also, though the decoupling capacitors are represented by lumped RLC circuits, they can be easily included in the system of equations. In order to construct passive reduced-order models, we utilize the ENOR algorithm. The accuracy of the proposed method is substantiated with some numerical examples.

2. Formulation of the Electromagnetic System

In the FDTD and FDFD methods, the Maxwell's curl equations are discretized spatially into the Yee's cell. **E** and **H** fields are separated in space according to the central difference approximation. The FDFD formulation proposed in [10] does not consider conductivity. On the other hand, the memory capacity for coefficient matrices required by [9] is 4 times as large as ones needed by [10]. Therefore, we adopt the formulation which took conductivity into consideration to [10].

In the proposed technique, eliminating **H** from the Maxwell's curl equations, we obtain the following form:

$$s\varepsilon \boldsymbol{E} + \sigma \boldsymbol{E} + \frac{1}{s\mu}\nabla\times\nabla\times\boldsymbol{E} = -\boldsymbol{J}, \tag{1}$$

where ε, μ and σ are the electrical permittivity, permeability and conductivity, respectively, and **J** is a source current density vector. By applying central differences to Eq. (1), the discretized expression in the z-direction is given by

$$\begin{aligned}
&s\varepsilon E_{z(i,j,k)} + \sigma E_{z(i,j,k)} \\
&+\frac{1}{s\mu}\left[\frac{1}{\Delta x}\left\{\frac{1}{\Delta z}\left(E_{x(i,j,k+1)} - E_{x(i,j,k)}\right) - \frac{1}{\Delta x}\left(E_{z(i+1,j,k)} - E_{z(i,j,k)}\right)\right\}\right. \\
&-\frac{1}{\Delta x}\left\{\frac{1}{\Delta z}\left(E_{x(i-1,j,k+1)} - E_{x(i-1,j,k)}\right) - \frac{1}{\Delta x}\left(E_{z(i,j,k)} - E_{z(i-1,j,k)}\right)\right\} \\
&-\frac{1}{\Delta y}\left\{\frac{1}{\Delta y}\left(E_{z(i,j+1,k)} - E_{z(i,j,k)}\right) - \frac{1}{\Delta z}\left(E_{y(i,j,k+1)} - E_{y(i,j,k)}\right)\right\} \\
&\left.+\frac{1}{\Delta y}\left\{\frac{1}{\Delta y}\left(E_{z(i,j,k)} - E_{z(i,j-1,k)}\right) - \frac{1}{\Delta z}\left(E_{y(i,j-1,k+1)} - E_{y(i,j-1,k)}\right)\right\}\right] \\
&= -J_{z(i,j,k)},
\end{aligned} \tag{2}$$

where Δx, Δy and Δz are the cell sizes in each direction, and (i, j, k) are position indices. Also the expression in the x-direction and the y-direction can be obtained in a similar way. As a result, the compact form of the discretized expressions becomes

$$\left(s\mathbf{D}_\varepsilon + \mathbf{D}_\sigma + \frac{\Psi}{s}\right)\mathbf{E}(s) = -\mathbf{B}_e\mathbf{J}_{in}, \tag{3}$$

where $\mathbf{D}_\varepsilon \in R^{3N\times 3N}$ and $\mathbf{D}_\sigma \in R^{3N\times 3N}$ are diagonal coefficient matrices, and $\Psi \in R^{3N\times 3N}$ becomes a symmetric matrix. Here, N denotes the total number of cells. $\mathbf{J}_{in} \in C^p$ is the vector of source current densities whose location is selected by the incidence matrix $\mathbf{B}_e \in R^{3N\times p}$.

3. Formulation of the Lumped RLC Elements and Circuits

3.1 Lumped RLC Elements

First, we assume that the lumped RLC element is located at a certain cell in the FDFD domain, and its device current I_L flows along the z-direction. At the cell corresponding to I_L, Eq. (2) becomes

$$s\varepsilon E_z + \frac{I_L}{\Delta x\Delta y} = \frac{I_{total}}{\Delta x\Delta y} \quad \text{or} \quad sC_0V_z + I_L = I_{total} \tag{4}$$

where

$$I_{total} = -\frac{\Delta x\Delta y}{s\mu}\nabla\times\nabla\times\mathbf{E}\Big|_z, \quad C_0 = \varepsilon\frac{\Delta x\Delta y}{\Delta z}, \quad V_z = E_z\Delta z. \tag{5}$$

Here C_0 is the equivalent capacitance of the cell. Since the branch equations of the RLC elements are given by

$$\left.\begin{aligned} I_L &= \frac{\Delta z}{R}E_z && resistor \\ I_L &= s\Delta z C E_z && capacitor \\ I_L &= -\frac{\Delta z}{sL}E_z && inductor \end{aligned}\right\} \tag{6}$$

it is easy to incorporate these lumped elements into the equations of the electromagnetic system.

3.2 Lumped RLC Circuits

Next, consider about incorporating a general linear lumped circuit into the system of equations. The n nodal equations for the network ϕ can be written as

$$\left(s\mathbf{C} + \mathbf{G} + \frac{\Gamma}{s}\right)\mathbf{X}(s) = \mathbf{B}_c\mathbf{I}_{in} + \mathbf{B}_{ec}I_L, \tag{7}$$

where $\mathbf{C} \in R^{n\times n}$, $\mathbf{G} \in R^{n\times n}$ and $\Gamma \in R^{n\times n}$ are nodal capacitance, resistance and susceptance matrices, which are symmetric and positive semi-definite, respectively. And the unknown vector $\mathbf{X} \in C^n$ denotes the nodal voltage vector. $\mathbf{I}_{in} \in C^p$ is the vector of source currents whose location is selected by the incidence matrix $\mathbf{B}_c \in R^{n\times p}$. Also I_L is a port current located at the connection node between the electromagnetic system and the lumped circuit. An element of the incidence vector $\mathbf{B}_{ec} \in C$

^{n} located at the connection node is set to 1, and others are set to 0. To combine Eq. (7) with the electromagnetic system, Eq. (7) is translated to the following equation:

$$\mathbf{B}_{ec}\frac{I_L}{\Delta x\Delta y}=\frac{\Delta z}{\Delta x\Delta y}\left(s\mathbf{C}+\mathbf{G}+\frac{\Gamma}{s}\right)\mathbf{E}_{\phi}(s)-\mathbf{B}_c\frac{\mathbf{I}_{in}}{\Delta x\Delta y}, \tag{8}$$

where $\mathbf{E}_{\phi}$ is the equivalent nodal electric-field vectors. An element of $\mathbf{E}_{\phi}$ located at the connection node is overlapped to the E_z of Eq. (4).

For example, in the case of Fig. 2, the KCL equation at the connection node can be written from Eq. (4) and Eq. (8) as

$$s\varepsilon E_z+\frac{\Delta z}{\Delta x\Delta y}(G_1+G_2)E_z-\frac{\Delta z}{\Delta x\Delta y}G_2E_2=\frac{I_{total}}{\Delta x\Delta y}. \tag{9}$$

Also the KCL equation at V_2 ($=E_2\Delta z$) is given by

$$-\frac{\Delta z}{\Delta x\Delta y}G_2E_z+\frac{\Delta z}{\Delta x\Delta y}(G_2+G_3)E_2=0. \tag{10}$$

Hence, these nodal equations can be combined with the whole system of equations.

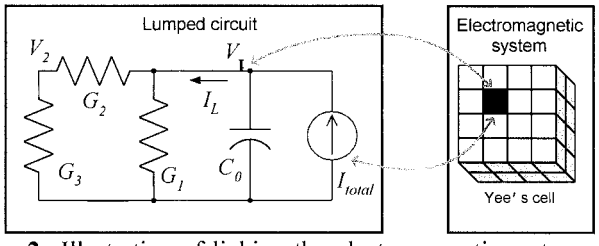

Fig. 2 Illustration of linking the electromagnetic system and the lumped circuit.

4. Model Order Reduction of the Hybrid Systems

We can solve the hybrid system of equations consisting of the electromagnetic system and the lumped RLC circuit at any frequency point by using variable iterative methods, such as the conjugate gradient (CG) method. However, this approach requires the huge memory capacity and the enormous CPU cost for the analysis of the large-scale PCB having complex structures, because of dividing the 3-dimensional region into a lot of minute cells. If we can make the macromodel of the hybrid system, the simulation including the electromagnetic effects of the PCB can be performed only by using a circuit simulator without solving repeatedly the large linear equation system. For this objective, we utilize the ENOR algorithm to construct passive reduced-order models.

The hybrid system of equations consisting of Eq. (3) and Eq. (7) is written as

$$\left(s\mathbf{C}_h+\mathbf{G}_h+\frac{\Gamma_h}{s}\right)\mathbf{E}(s)=\mathbf{B}_h\mathbf{J}_h, \tag{11}$$

where $\mathbf{C}_h\in R^{M\times M}$ is the permittivity matrix, $\mathbf{G}_h\in R^{M\times M}$ is the conductivity matrix, and $\Gamma_h\in R^{M\times M}$ is the matrix described by permeability and susceptance ($M=3\times N+n-1$). $\mathbf{J}_h\in C^P$ is the vector of source current densities whose location is selected by the incidence matrix $\mathbf{B}_h\in R^{M\times P}$. The impedance transfer function is given by

$$\boldsymbol{Z}(s)=\boldsymbol{B}_{hO}^T\left(s\boldsymbol{C}_h+\boldsymbol{G}_h+\frac{\Gamma_h}{s}\right)^{-1}\boldsymbol{B}, \tag{12}$$

where $\mathbf{B}_{hO}\in R^{M\times P}$ is the incidence matrix to select the location of output ports. Using the ENOR algorithm, the orthogonal projection matrix $\mathrm{V}\in R^{M\times m}$ can be obtained. As a result, the projected system is written by

$$\widetilde{\boldsymbol{Z}}(s)=\widetilde{\boldsymbol{B}}_{hO}{}^T\left(s\widetilde{\boldsymbol{C}}_h+\widetilde{\boldsymbol{G}}_h+\frac{\widetilde{\Gamma}_h}{s}\right)^{-1}\widetilde{\boldsymbol{B}}_h, \tag{13}$$

where

$$\widetilde{\mathbf{C}}_h=\mathbf{V}^T\mathbf{C}_h\mathbf{V},\qquad \widetilde{\mathbf{G}}_h=\mathbf{V}^T\mathbf{G}_h\mathbf{V},\qquad \widetilde{\Gamma}_h=\mathbf{V}^T\Gamma_h\mathbf{V},$$
$$\widetilde{\mathbf{B}}_h=\mathbf{V}^T\mathbf{B}_h. \tag{14}$$

and

$$\widetilde{\boldsymbol{B}}_{hO}=\boldsymbol{V}^T\boldsymbol{B}_{hO} \tag{15}$$

In the projected system, only dominant system eigenvalues are selected, and the others are ignored. Because m is much smaller than M, it is easy to solve the reduced-order model by using the direct methods, such as the LU decomposition.

Additionally, Eq. (13) is rewritten as

$$\widetilde{\boldsymbol{Z}}(s)=\widetilde{\boldsymbol{B}}_{hO}^T H_h(s) \tag{16}$$

where

$$H_h(s)=\left(s\widetilde{\boldsymbol{C}}_h+\widetilde{\boldsymbol{G}}_h+\frac{\widetilde{\Gamma}_h}{s}\right)^{-1}\widetilde{\boldsymbol{B}}_h. \tag{17}$$

If we only calculate the matrix $\mathbf{H}_h$(s) from Eq. (17) at arbitral frequency point s (= $j\omega$) in advance, a response at every port can be obtained by changing selection of $\mathbf{B}_{hO}$ which implies the location of the output port and calculating Eq. (15) and Eq. (16). Therefore, this is effective in the case of analyzing the power plane resonance, because generally 2-dimentional electrical field distributions between the power/GND planes are often calculated in that case.

5. Numerical Results

We have simulated an example circuit board which is shown in [13] in order to verify the validity of the proposed method. The example is a 10cmX10cm 2-layered printed board, which is constructed by the power distribution and the ground planes. In [13], the measurement and FDTD simulation results have been already shown. It is assumed that the relative permittivity of PCB is 4.0. Then, the impedance at the output port at (x, y)=(5cm, 2cm) was simulated in the case that the current source is added at (x, y)=(5cm, 4cm). The obtained impedances at the output port are illustrated in Fig.3, where 25 poles model was used as the reduced macromodel. From Fig.3, we can see that the simulation results obtained by the present method give the good agreement with the ones in [13].

In general, a low power supply impedance is required at a wide frequency range for the high-speed circuit design. The basic approach for keeping the impedance low is to place

bypass capacitors between the power/GND planes. Therefore, we have simulated the PCB with 16 bypass capacitors around the current source. Here, the bypass capacitor is modeled as the equivalent circuit including ESR and ESL. The simulation results are also shown in Fig.3. From Fig.3, we can see that the power resonances can be inhibited around at 750MHz. Furthermore, electric field distributions on 2-dimensional plane have been computed and the results are illustrated in Fig.4. From Fig.4, we can see that the plane resonances can be inhibited by the bypass capacitors.

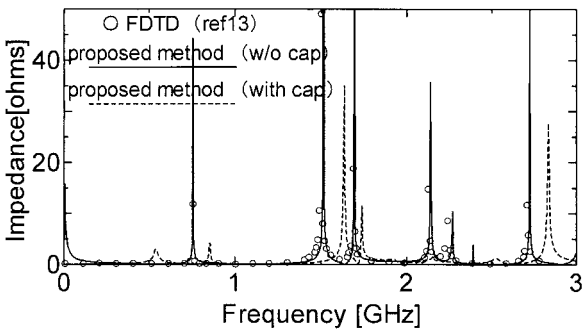

Fig. 3 Impedance characteristics.

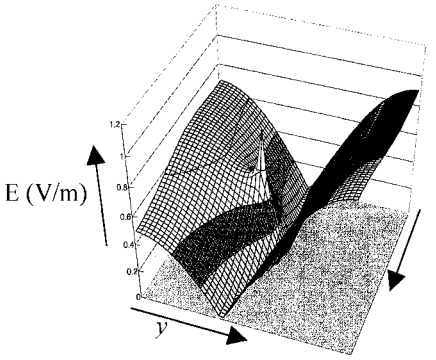

(a) without bypass capacitors.

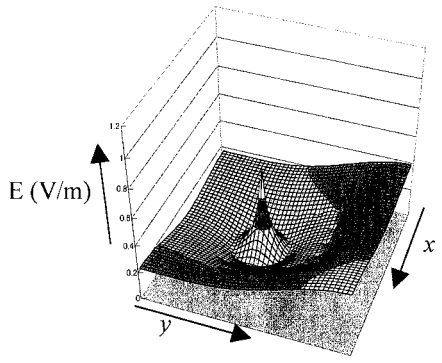

(b) with bypass capacitors.

Fig. 4 Electric field distributions between planes.

6. Conclusions

We have presented a model order reduction technique for the hybrid systems which are composed of electromagnetic systems and lumped RLC circuits. Differently from the PEEC method, our method does not need the complicated process, such as the 3-D parameter extraction. Finally, we have shown the validity of the present technique. Although the bypass capacitors are modeled as the lumped RLC circuits, our method can treat them without any problems.

References

[1] H. Heeb and A.E. Ruehli, "Three-dimensional Interconnect analysis using partial element equivalent circuits," IEEE Trans. Circuits & Systems-I, vol.39, pp.974-982, Nov. 1992.

[2] B. Archambeault and A.E. Ruehli, "Analysis of Power/Ground-Plane EMI Decoupling Performance Using the Partial-Element Equivalent Circuit Technique," IEEE Trans. Electromagnetic Compatibility, vol. 43, no. 4, pp.437-445, Nov. 2001.

[3] K.S. Yee, "Numerical solution of initial boundary value problems involving Maxwell's equations in isotropic media," IEEE Trans. Antennas Propagation, vol.14, no.5. pp. 302-307, 1966.

[4] D.M. Sheen, et al., "Application of the three-dimensional finite-difference time-domain method to the analysis of planar microstrip circuits," IEEE Trans. Microwave Theory & Tech., vol.38, no.7, pp.849-857, 1990.

[5] W.T. Beyene and J. Schutt-Aine, "Efficient transient simulation of high-speed interconnects characterized by sampled data," IEEE Tran. Comps., Pack., Manuf. Technol. -Part B, vol.21, no.1, Feb. 1998.

[6] M. Suzuki, H. Miyashita, A. Kamo, T. Watanabe, and H. Asai, "A Synthesis Technique of Time-Domain Interconnect Models by MIMO Type of Selective Orthogonal Least-Square Method," IEEE Trans. Microwave Theory & Tech., vol.49, no.10, pp.1708-1714, Oct. 2001.

[7] R. Achar, P.K. Gunupudi, M.S. Nakhla, and E. Chiprout, "Passive interconnect reduction algorithm for distributed/measured networks," IEEE Trans. Microwave Theory & Tech., vol.47, no.4, pp.287-301, April 2000.

[8] J. Morsey and A.C. Cangellaris, "PRIME: Passive Realization of Interconnect Models from Measured Data," Proc. IEEE EPEP2001, Oct. 2001.

[9] A.C. Cangellaris, M. Celik, S. Pasha, and L. Zhao, "Electromagnetic Model Order Reduction for System-Level Modeling," IEEE Trans. Microwave Theory & Tech., vol.47, no.6, pp.840-850, 1999.

[10] L. Kulas and M. Mrozowski, "Reduced-Order Models in FDTD," IEEE Microwave and Wireless Comp. Letters, vol. 11, No. 10, pp.422-424, Oct. 2001.

[11] A. Odabasioglu, M. Celik, and L.T. Pileggi, "PRIMA: Passive Reduced-order Interconnect Macromodeling Algorithm," Proc. ICCAD'97, pp.58-65, Nov. 1997.

[12] B.N. Sheehan, "ENOR: Model Order Reduction of RLC Circuits Using Nodal Equations for Efficient Factorization," Proc. DAC'99, pp. 17-21, 1999.

[13] S.Van den Berghe, F.Olyslager, D.De Zutter, J.De Moerloose and W.Temmerman, "Study of the Ground Bounce Caused by Power Plane Resonances", IEEE Trans. On Electromagnetic Compatibility, vol.40, no.2, May 1998.